Biochemical Engineering Journal 114 (2016) 226–236

Contents lists available at ScienceDirect

Biochemical Engineering Journal

journal homepage: www.elsevier.com/locate/bej

Regular article

Modelling of batch kinetics of aerobic carotenoid production using *Saccharomyces cerevisiae*

M. Carolina Ordoñez, Jonathan P. Raftery, Tejasvi Jaladi, Xinhe Chen, Katy Kao, M. Nazmul Karim*

Artie McFerrin Department of Chemical Engineering, Texas A&M University, College Station, TX 77840, USA

ARTICLE INFO

Article history:
Received 5 March 2016
Received in revised form 14 June 2016
Accepted 3 July 2016
Available online 14 July 2016

Keywords:
Batch processing
β-Carotene
Modelling
Yeast cultivation
Sensitivity analysis

ABSTRACT

Carotenes such as β-carotene have a positive impact in human health as a precursor of vitamin A. The structural complexity of these compounds makes chemical synthesis a difficult option, facilitating the need for their biological production. Reliable mathematical models for batch cultivation are developed to describe the glucose consumption, product formation and depletion, and β-carotene production of the *Saccharomyces cerevisiae* strain mutant SM14 with 20 g/L glucose as the carbon source. Parameter estimation for the models employ an objective function minimizing an expression that uses the coefficient of determination R^2, which avoids the necessity of weighting or normalizing the equations. Comparison with experimental data shows that the developed models show a satisfactory prediction of the overflow metabolism that is happening in the cell. Additionally, local and global sensitivity analysis of the models with respect to the optimal parameters is also studied and further show that the models developed here accurately describe trends in the dynamic states of the bioreactor during batch fermentation.

1. Introduction

Carotenoids, a diverse group of yellow-orange pigments found in many biological systems, are produced by diverse organisms such as plants, fungi, and bacteria [1–3]. Because of its colored characteristic, it has been extensively used in food pigmentation and as constituents in vitamins and dietary supplements [4–7]. Carotenes, such as β-carotene, have important biological roles as a precursor of vitamin A. They have been shown to have positive impacts in human health, having antioxidant effects and properties protective against cancer [8–11].

Presently, some carotenoids are industrially produced by synthetic chemical technology; however some of the by-products have undesirable side effects when consumed and most of the carotenoids such as β-carotene have a structural complexity that makes the chemical synthesis an unviable option. For this reason, the production of carotenoids from microbial sources has been the focus of vast literature references [4,12–15].

Overflow metabolism is the incomplete oxidation of the carbon source resulting in the excretion of generally inhibitory organic end products during aerobic operations. This phenomenon, also called the "short-term Crabtree effect", manifests usually at a high substrate concentration [16,17]. Various microorganisms exhibit this phenomena, examples of which include *Saccharomyces cerevisiae* cultures with aerobic ethanol formation [18,19], *Escherichia coli* cultures with aerobic acetate formation [20,21], or mammalian cell cultures with aerobic lactate formation [22]. This inhibition effect is undesirable in many processes and leads to complications when trying to quantitatively describe these systems.

Mathematical models describing the kinetics of microbial growth, substrate uptake and product formation are very useful for optimization, process control, the reduction of process operating costs, and the increase of product quality of cultivation processes. In this context, kinetic models have been reported for yeast systems such as *Xanthophyllomyces dendrorhous* [23,24] but there are very few studies dealing with appropriate modelling approach for engineered *S. cerevisiae* strains, and more specifically those engineered for the production of β-carotene. The aim of this work is to develop a suitable and reliable kinetic model for the β-carotene production in batch cultures of an engineered *S. cerevisiae* strain using glucose as the main substrate. This model is also applied to predict cell growth, substrate consumption, ethanol and acetic acid formation and later assimilation. Furthermore, sensitivities of various model parameters were studied to elucidate the need to focus on key model parameters.

* Corresponding author.
E-mail address: nazkarim@tamu.edu (M.N. Karim).

http://dx.doi.org/10.1016/j.bej.2016.07.004
1369-703X/

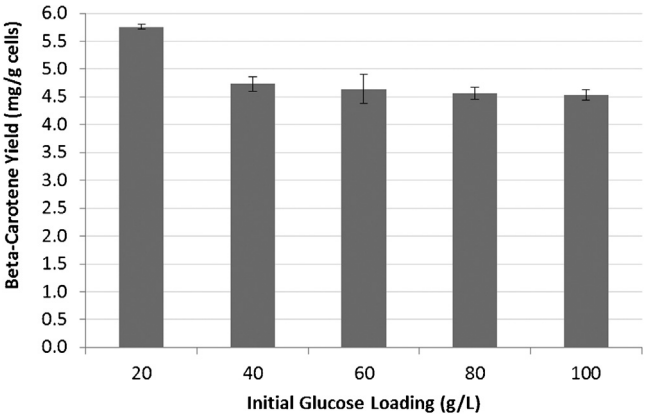

Fig. 1. Effect of initial glucose concentration on overall carotenoid yield. Experiments were done in YPD media with varying concentrations of glucose (20 g/L, 40 g/L, 60 g/L, 80 g/L and 100 g/L), were inoculated in a 1:60 ratio, and were grown at 200 rpm and 30 °C for 110 h after innoculation to allow for complete use of glucose.

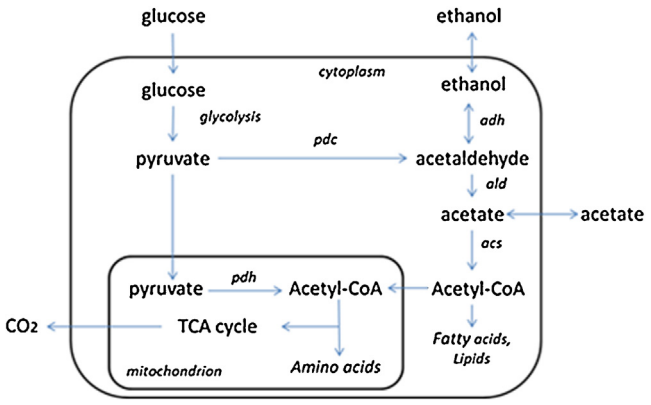

Fig. 2. Overview of the metabolic pathways found in wild type *S. cerevisiae*. The key enzymes for overflow metabolism are: pdh: pyruvate dehydrogenase complex; pdc: pyruvate decarboxylase; adh: alcohol dehydrogenase; ald: acetaldehyde dehydrogenase; acs: acetyl coa synthetase.

2. Materials and methods

2.1. Microorganism and culture media

An *S. cerevisiae* strain mutant SM14 engineered to produced β-carotene was used in this study [25]. The yeast strain was stored in frozen vials at −80 °C and in plates at 4 °C which were subcultured every three weeks for maintenance. Experiments were conducted to determine the optimal initial glucose loading for all experiments. A single flask of 50 mL YPD and 20 g/L glucose was inoculated with a single colony and grown at 200 rpm and 30 °C overnight until the exponential growth phase was reached. Using this culture, YPD media with varying concentrations of glucose (20 g/L, 40 g/L, 60 g/L, 80 g/L and 100 g/L) were inoculated in a 1:60 ratio that was intended for the bioreactor studies. These shake flask cultures were grown at 200 rpm and 30 °C for 110 h after innoculation to allow for complete utilization of glucose. The beta-carotene concentrations were analyzed at the end of this time to determine the optimal initial glucose concentration that would yield the highest amount of β-carotene per gram of cells. Fig. 1 below shows the productivity results of these experiments.

The results in Fig. 1 show that an increase in initial glucose concentration shows an inverse relationship with the overall β-carotene yield on a gram-dry-cell-weight basis. Based on these results, it was determined that 20 g/L was optimal initial glucose loading. As such, all experiments were conducted with the cells grown in fresh Yeast Nitrogen Base (YNB) media supplemented with 20 g/L D-glucose.

2.2. Bioreactor cultivation studies

The bioreactor studies were carried out in a 7 L, glass, autoclavable bioreactor (Applikon®, Foster City, CA) with a 3 L working volume. The bioreactor was inoculated with the entire seed culture. The temperature was set at 30 °C, pH was maintained at 4 by addition of 2 M HCL or 2 M NaOH as needed, the agitation speed was kept constant at 800 rpm and the bioreactor was supplied with a constant airflow of 6 L/min. These conditions were optimized experimentally by Olson [26]. All the bioreactor experiments were performed in batch mode carried out in duplicate with duration of 72 h, the time at which the acetic acid produced was totally consumed. Substrate consumption and product formation and depletion were verified using the HPLC Agilent Technologies 1290 Infinity with the use of the Aminex HPX-87H HPLC column.

The *S. cerevisiae* SM14 culture presents the following characteristics in a stirred-tank bioreactor with 20 g/L initial glucose. Initially, ethanol and acetic acid are produced in the early stage of the batch culture due the overflow metabolism. The production of these metabolites starts with glycolysis, the metabolic pathway where the six-carbon glucose molecule is broken down into two three-carbon pyruvate molecules. At this level, cell respiration via the mitochondrial pyruvate dehydrogenase complex (*pdh*) producing Acetyl-CoA competes with cytosolic pyruvate decarboxylase (*pdc*) reducing it to acetaldehyde [27–30]. Once the acetaldehyde is formed through the pyruvate decarboxylase activity, it may feed the tricarboxylic acid cycle (TCA), reducing the acetaldehyde via acetaldehyde dehydrogenase (*ald*) to acetate and then producing acetyl coenzyme A (Acetyl-CoA) through acetyl-CoA synthetase (*acs*) [30,31]. Alternatively, acetaldehyde is reduced to ethanol instead of being oxidized to carbon dioxide thru alcohol dehydrogenase (*adh*) [27], as shown in Fig. 2. When the glucose is consumed, the ethanol present in the medium can be utilized via aerobic metabolism and converted to Acetyl-CoA via acetaldehyde and acetate, the pathway does not proceed via pyruvate. Similarly, once the ethanol becomes exhausted the acetate can be consumed [32].

The produced acetyl coenzyme A can be used in many different biochemical reactions such as the mevalonate pathway shown in Fig. 3. Beta-carotene is derived from the isopentenyl diphosphate (IPP) and dimethylallyl diphosphate (DMAPP) which can be condensed into geranyl pyrophosphate (GPP), a C_{10} molecule, and is then converted to the C_{15} molecule farnesyl pyrophosphate (FPP) with the addition of an isoprene unit. The FPP is condensed into geranylgeranyl pyrophosphate (GGPP), a C_{20} compound, catalyzed by *crtE*. The β-carotene biosynthesis starts with the formation of the C_{40} carotenoid phytoene, catalyzed by phytoene synthase (*crtYB*). Isomerization and desaturation reactions allow the formation of lycopene, which forms β-carotene [33–35]. These pathways, highlighted in red in Fig. 3 below, are not native and were introduced to the genome recombinantly.

2.3. Inhibition studies

Experiments were performed to determine if the products inhibit the growth rate of the *S. cerevisiae* SM14. The experiments were done in a baffled Erlenmeyer flask containing with 50 mL of YNB media and incubated for 24 h at 30 °C in a shaker at 200 rpm. Cell growth was measured in terms of turbidity at 600 nm. To measure the inhibition effects of the products, e.g. ethanol and acetic acid, experiments were run with 20 g/L of glucose and various con-

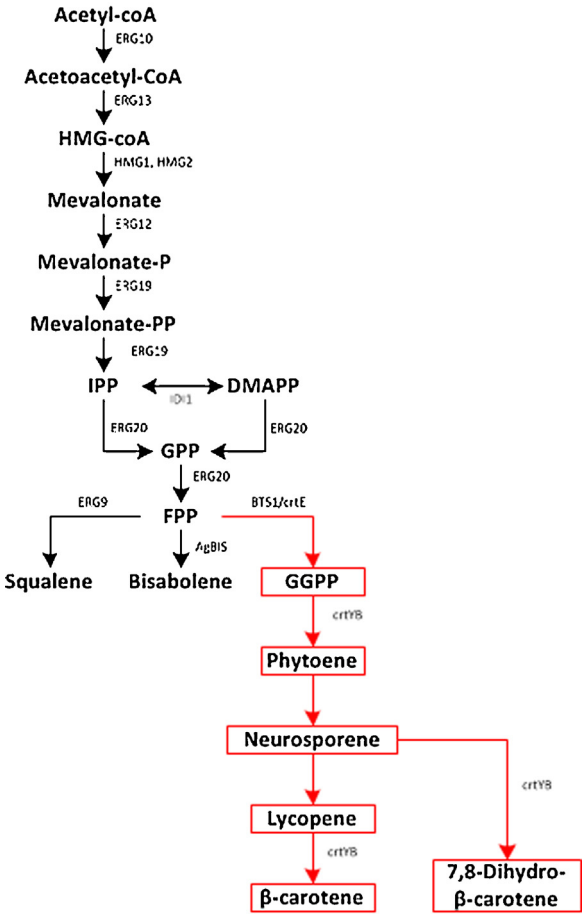

Fig. 3. Mevalonate pathway genetically engineered via chromosomal integration into the *S. cerevisiae* SM14 strain. The β-carotene synthesis pathway introduced to the genome recombinantly, is highlighted in red [33]. (For interpretation of the references to color in this figure legend, the reader is referred to the web version of this article.)

centrations of the ethanol and acetic acid products. The ethanol concentration was varied from 0 to 70 g/L and the acetic acid from 0 to 10 g/L, as described in Maiorella et al. [36]. The maximum growth rate was calculated for each experiment and plotted as a function of the ethanol or acetic acid initial concentration.

2.4. Analytical methods

Cell growth was monitored based on an increase in the OD_{600} of the culture. For the β-carotene quantification the cells were disrupted using the method described by Reyes et al. [25]. The D-glucose, ethanol and acetic acid concentrations in the media were analyzed by HPLC.

2.5. Kinetic modeling strategy

2.5.1. Kinetic model

In view of the characteristics of the system and based on literature, a model was proposed to describe the overflow metabolism with the depletion of ethanol and acetic acid.

As glucose, ethanol and acetic acid can be utilized for biomass production, the cell growth rate can be represented by

$$\frac{dX}{dt} = (\mu_G + \mu_E + \mu_A)X \tag{1}$$

where μ_G, μ_E and μ_A represent the specific growth rate on glucose, ethanol and acetic acid respectively. The Monod equation is the most common unstructured kinetic model for microbial growth, which relates the microbial growth rate to a single limiting substrate [36]. When the medium contains more than one carbon source multiple lag phases may be observed, caused by a shift in metabolic pathways in the growth cycle, a phenomenon called "diauxic growth" by Monod [38]. For mixed substrates, the model requires a modification as described by Yoon et al.

$$\mu = \mu_G + \mu_E + \mu_A \tag{2}$$

$$\mu_G = \left(\frac{\mu_{\max,G} \cdot \chi_E \cdot \chi_A \cdot G}{K_{SG} + G + a_{ge}E + a_{ga}A}\right) \tag{3a}$$

$$\mu_E = \left(\frac{\mu_{\max,E} E}{K_{SE} + E + a_{eg}G + a_{ea}A}\right) \tag{3b}$$

$$\mu_A = \left(\frac{\mu_{\max,A} A}{K_{SA} + A + a_{ag}G + a_{ae}E}\right) \tag{3c}$$

where a_{ij} represents the inhibition effect of the jth substrate on the utilization of the ith substrate by the organism [39]. If $a_{ij} = 1$, the jth substrate has the same inhibition effect as the ith substrate itself on the ith substrate utilization. If $a_{ij} > 1$, the jth substrate has inhibition on the ith substrate utilization. If a_{ij} is much greater than 1, the jth substrate has a repression effect on the utilization of the ith substrate by the microorganism. $\mu_{\max,G}$, $\mu_{\max,E}$, and $\mu_{\max,A}$ are the maximum specific growth rates on glucose, ethanol and acetic acid, respectively. The variables G, E and A are the glucose, ethanol and acetic acid concentrations. The variables χ_E and χ_A are added to $\mu_{\max,G}$ to account for any effect of ethanol or acetic acid inhibition on the glucose growth rate. These variables are functions of the ethanol and acetic acid concentration, respectively, whose functionalities are determined using the inhibition studies discussed in Section 2.3.

The mass balance for substrate governs the production of biomass. The energy requirement for cellular maintenance is very small relative to that of growth [24], and for that reason it is neglected in the mass balance calculations. Then, the glucose consumption rate is given by Eq. (4), where $Y_{X/G}$ is the biomass yield coefficient on glucose.

$$\frac{dG}{dt} = -\frac{\mu_G X}{Y_{X/G}} \tag{4}$$

The ethanol production from fermentative catabolism of glucose occurs during the exponential growth phase and is growth associated [37,40], hence ethanol formation is related to the yeast growth on glucose, shown by the first term of Eq. (5). The second term represents the amount of ethanol that is consumed by the yeast cells, where $Y_{X/E}$ is the biomass yield coefficient on ethanol.

$$\frac{dE}{dt} = k_1 \mu_G X - \frac{\mu_E X}{Y_{X/E}} \tag{5}$$

Similarly, the acetic acid model takes into account the amount produced by the consumption of glucose and ethanol as well as the acetic acid consumed by the yeast cells, where $Y_{X/A}$ is the biomass yield coefficient on acetic acid. We assumed that the acetic acid formation occurred in the growth phase of the cells.

$$\frac{dA}{dt} = (k_2 \mu_G + k_3 \mu_E)X - \frac{\mu_A X}{Y_{X/A}} \tag{6}$$

Carotenoid production in *X. dendrorhous* yeast cultures is partially growth associated, occurring in both the growth and stationary phase [40]. As the genes incorporated into the *S. cerevisiae* SM14 strain of interest came from an *X. dendrorhous* strain, it is assumed that the recombinant yeast would follow the same behavior. Therefore, β-carotene production can be related to cell growth and biomass concentration by the Luedeking-Piret equation

given in Eq. (7), where α_i represents the coefficients for growth-associated product formation related to the yeast growth on each substrate, and β is the coefficient for non-growth-associated carotenoid production [42].

$$\frac{dP}{dt} = (\alpha_1\mu_G + \alpha_2\mu_E + \alpha_3\mu_A)X + \beta X \tag{7}$$

2.5.2. Parameter estimation

In the previous section we have developed five dynamic model equations for cell growth (Eq. (1)), substrate consumption (Eq. (4)), ethanol and acetic acid formation and depletion (Eqs. (5) and (6)) and β-carotene production (Eq. (7)). This section will explain how the parameters of these model equations were estimated from experimental data. The parameter estimation is done in two steps, first to determine the optimal parameters in the growth rate equations and then to find the optimal parameters in the dynamic model equations using the determined growth rate parameters. Values used to initialize the two parameter estimation algorithms were selected from literature for the growth of *S. cerevisiae* and *X. dendrorhous* [24,41,43].

The data used in estimating the parameters of the model were filtered using a cubic smoothing spline method, a piecewise function that has a high degree of "smoothness", available in Matlab [44]. From the batch cultivation data, we can distinguish three different growth rates related to the substrate that is being consumed at any particular moment in the cultivation. The specific growth rate expression is a generalized Monod model for the growth of an organism on mixed substrates (Eqs. (2) and (3)). Specific growth rate μ was calculated as

$$\mu = \frac{\ln\left(\frac{x_2}{x_1}\right)}{t_2 - t_1} \tag{8}$$

With the collected data and the developed parameter estimation algorithm, the optimal parameters were estimated for the specific growth rate. The objective function used is the sum of squared errors (SSE) between the known data and model predictions and uses the Matlab *fmincon* function.

To estimate the parameters of the dynamic mass balance equations, we propose the use of an expression that minimizes the coefficient of determination, R^2, as the objective function. The R^2 is a value that ranges from zero to unity and indicates the "goodness" of the fit between the model and the data. Using this value, the objective function avoids the necessity of weighting the equations, a common method found in the literature due to the order of magnitude difference in the expected concentrations of carotenoids versus the other products [24].

Knowing that the best R^2 value for each curve to be unity, the objective function for the second optimization is shown in Eq. (9), where the coefficient of determination was calculated for each variable of the system.

$$\min Z = 5 - \left(R_p^2 + R_x^2 + R_s^2 + R_e^2 + R_a^2\right) \tag{9}$$

Eq. (10) shows how each R^2 value is calculated, where the sum of the square error (SSE) is given by Eq. (11), Δ_i^2 being the squared difference between the data value and the predicted value at a given time point. Eq. (12) represents the total of sum squares (SST) which is the difference between the value to be predicted and the arithmetic mean of the observed data.

$$R^2 = \frac{1}{m}\sum_{j=1}^{m}\left(1 - \frac{SSE}{SST}\right) \tag{10}$$

$$SSE = \sum_{i=1}^{n}\Delta_i^2 \tag{11}$$

$$SST = \sum_{i=1}^{n}(y_i - \bar{y})^2 \tag{12}$$

The constraints of this optimization problem are the 5 dynamic mass balances describing the concentration of each component in the system. This programming problem is solved by setting the parameters optimized in the growth rate equations and using an iterative looping method that passes between the *fmincon* algorithm and *ode45* algorithm found in Matlab to estimate the remaining parameters. Fig. 4 summarizes the steps that the parameter estimation algorithm takes to calculate the optimal value for the differential equations that describes our system.

2.5.3. Local sensitivity analysis – direct differential method

Local sensitivity analysis is the analysis of the output of a set of models with respect to small perturbations in the model parameters or initial conditions. One of the most widely used methods for doing this analysis is the calculation of sensitivity indices, *S*, via the direct differential method. Calculation of these sensitivity indices requires the development of differential equations of the sensitivity index, shown in Eq. (13), which include calculations of the Jacobian matrix of the system as well as the derivative of each model with respect to the parameter or initial condition of interest [45]. The definition of the Jacobian matrix $\boldsymbol{J}$, sensitivity index vector $\boldsymbol{S}$, and vector of function-parameter derivatives $\boldsymbol{F_j}$ is shown in Eq. (14). This results in a large scale system of differential equations which need to be solved simultaneously with the initial conditions shown in Eq. (15).

$$\frac{d}{dt}\frac{\partial \boldsymbol{y}}{\partial p_j} = \frac{\partial \boldsymbol{f}}{\partial \boldsymbol{y}}\frac{\partial \boldsymbol{y}}{\partial p_j} + \frac{\partial f}{\partial p_j} = \boldsymbol{J}*\boldsymbol{S_j} + \boldsymbol{F_j} \tag{13}$$

$$J = \frac{\partial \boldsymbol{f}}{\partial \boldsymbol{y}} = \begin{bmatrix} \frac{\partial f_1}{\partial y_1} & \frac{\partial f_1}{\partial y_2} & \cdots & \frac{\partial f_1}{\partial y_n} \\ \frac{\partial f_2}{\partial y_1} & \frac{\partial f_2}{\partial y_2} & & \frac{\partial f_2}{\partial y_n} \\ \vdots & & \ddots & \vdots \\ \frac{\partial f_n}{\partial y_1} & \frac{\partial f_n}{\partial y_2} & \cdots & \frac{\partial f_n}{\partial y_n} \end{bmatrix}, \quad \boldsymbol{S} = \frac{\partial \boldsymbol{y}}{\partial p_j} = \begin{bmatrix} S_{1,j} \\ S_{2,j} \\ \cdots \\ S_{n,j} \end{bmatrix}, \quad \boldsymbol{F}_j = \frac{\partial f}{\partial p_j} = \begin{bmatrix} \frac{\partial f_1}{\partial p_j} \\ \frac{\partial f_2}{\partial p_j} \\ \cdots \\ \frac{\partial f_n}{\partial p_j} \end{bmatrix} \tag{14}$$

$$\text{At } t = 0, s\left(y_n, y_n^i\right) = 1; s\left(y_n, p_j\right) = 0; s\left(y_n, y_{n\pm1}^i\right) = 0 \tag{15}$$

The kinetic models used to describe the carotenoid production by *S. cerevisiae* SM14 above consist of 5 ordinary differential equations, 5 initial conditions, and 10 variables of interest. To implement the direct differential method described above, equations were developed for 75 total sensitivity indices. These equations were solved simultaneously and the results were analyzed to determine the parameters most important to each model equation when small perturbations are considered.

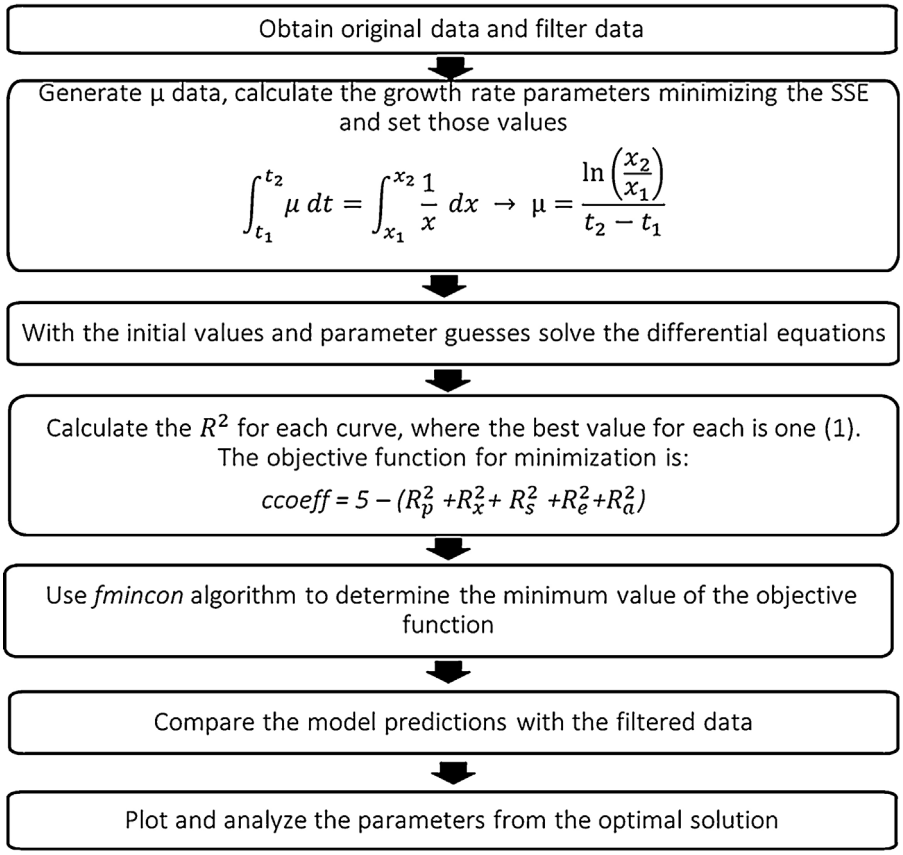

Fig. 4. Optimization scheme used to determine the optimal parameters of the batch kinetic model.

2.5.4. Global sensitivity analysis – ANOVA method

While local sensitivity analysis looks at the sensitivity of a solution in a close proximity to the optimal solution, it is also worth analyzing the sensitivity of the models for the full range of possible parameter values. For this, global sensitivity analysis can be used, which instead of considering only small perturbations in one parameter at a time focuses on parameter variations over the entire possible parameter space. In addition, global sensitivity indices can examine the combined effect of multiple parameters on the model solutions. Unlike local sensitivity analysis, which considers the sensitivity of the model subject to the nominal optimal parameters, the global sensitivity analysis considers the sensitivity of the model over the entire feasible space of the parameters. Consequently, the calculated global sensitivity indices allow the study of the mathematical model rather than a specific solution.

The method used for calculating the global sensitivity index relies upon stochastic variations of parameters. The method uses a normally distributed search of the parameter space and subsequent analysis of the variance (ANOVA) in the model outputs [46]. This is called the ANOVA method and utilizes a Monte Carlo search method to produce a large number ($2N > 10,000$) of parameter inputs (γ).

$$\xi_j = \left(\gamma_1^j, \ldots, \gamma_{2N}^j\right)$$

The large number of sample points is then split into two matrices of equal size, denoted by ξ_j and ξ_j' below. These two matrices will be the basis for the calculation of the global sensitivity indices.

$$\xi_j = \left(\gamma_1^j, \ldots, \gamma_N^j\right) = \left(\eta_j, \zeta_j\right)$$

$$\xi_j' = \left(\gamma_{N+1}^j, \ldots, \gamma_{2N}^j\right) = \left(\eta_j', \zeta_j'\right)$$

To begin the algorithm, the rows belonging to the individual variable or combination of variables of interest are swapped between the matrices ξ_j and ξ_j', as shown below.

$$\xi_j^* = \left(\eta_j, \zeta_j'\right) \quad \xi_j'^* = \left(\eta_j', \zeta_j\right)$$

The equations are solved with each parameter set found in the matrices ξ_j and ξ_j^*, and are given by $f\left(\xi_j\right)$ and $f\left(\xi_j^*\right)$ in Eqs. (16) through (18). Using the model outputs it is possible to calculate their variances with respect to the original data set, the set of variables of interest, denoted by$y$, and the set of all other parameters, denoted by z, using Eqs. (16) through (19).

$$\frac{1}{N}\sum_{j=1}^{N} f\left(\xi_j\right) \xrightarrow{P} f_0^2 \tag{16}$$

$$\frac{1}{N}\sum_{j=1}^{N} f^2\left(\xi_j\right) \xrightarrow{P} D + f_0^2 \tag{17}$$

$$\frac{1}{2N}\sum_{j=1}^{N} \left[f\left(\xi_j\right) - f\left(\xi_j^*\right)\right]^2 \xrightarrow{P} D_z^{tot} \tag{18}$$

$$D_y = D - D_z^{tot} \tag{19}$$

With the variances known it is possible to calculate two global sensitivity indices for the variable set of interest. This is done by using Eqs. (20) and (21). The first global sensitivity index, S_y, is a

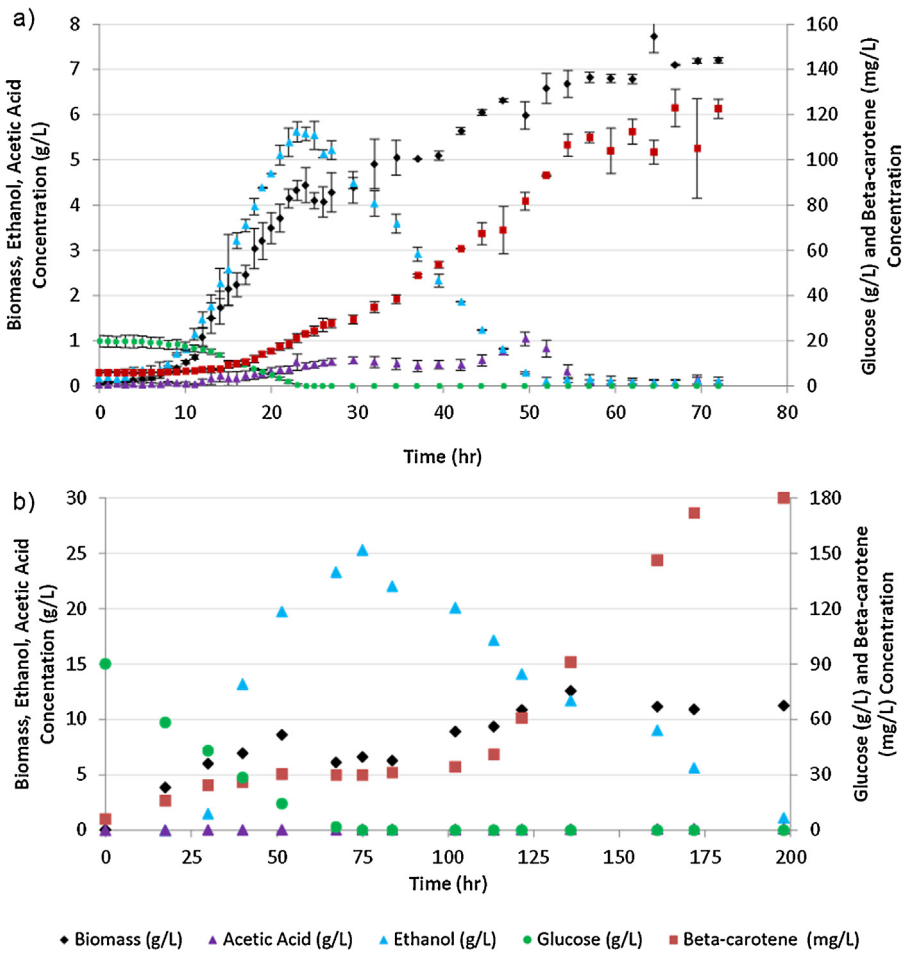

Fig. 5. Time courses of cell growth, glucose consumption, ethanol and acetic acid concentration and carotenoids production in batch cultures of *S. cerevisiae* with (a) 20 g/L initial glucose and (b) 90 g/L glucose. Experiments with 20 g/L glucose were repeated twice, with samples taken in duplicate for each.

measure of the sensitivity of the model with respect to only the single variable of interest. For example, $S_{G,Y_{XG}}$ would denote the sensitivity of the glucose model with respect to only the Y_{XG} parameter. The second sensitivity index, S_Y^{tot}, is the measure of the total sensitivity that a model has to a parameter y. Unlike the first index, S_y, this second index also accounts for the variance associated with interactions between all parameters and the parameter of interest, thus accounting for the total variance associated with parameter y. To contrast with $S_{G,Y_{XG}}$, the sensitivity index $S^{tot}_{G,Y_{XG}}$ would account for the sensitivity of not only $S_{G,Y_{XG}}$ but also of the sensitivity of any combination of parameters combined with Y_{XG}.

$$S_y = \frac{D_y}{D} \tag{20}$$

$$S_y^{tot} = \frac{D_y^{tot}}{D} \tag{21}$$

These sensitivity indices can have values between zero and unity. While intermediate values of these are not necessarily informative, there are a few extreme cases which can divulge how the model and parameters interact [47]:

1. If $S_y = S_y^{tot}$, the variable of interest is not involved in any interaction with other input factors.
2. If $S_y = S_y^{tot} = 0$, the model does not depend on the variable of interest.
3. If $S_y = S_y^{tot} = 1$, the model depends only on the variable of interest.

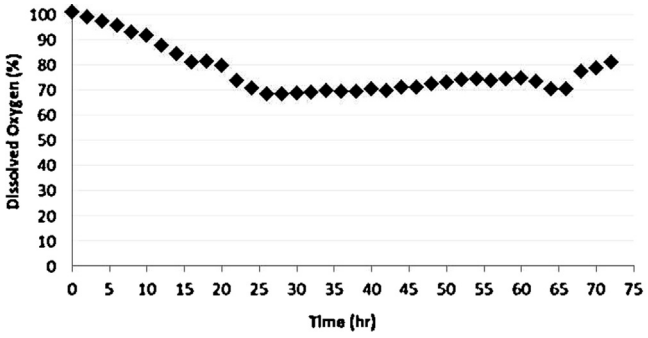

Fig. 6. The dissolved oxygen profile for a batch culture of *S. cerevisiae* with 20 g/L initial glucose.

3. Results and discussion

3.1. Bioreactor cultivation results

Fig. 5a shows the batch culture profiles of the cell growth, β-carotene production, ethanol and acetic acid production and subsequent consumption, and glucose consumption of *S. cerevisiae* SM14 in a stirred-tank bioreactor with 20 g/L initial glucose. Fig. 6 shows the time profile for the dissolved oxygen content in the bioreactor as a percentage of the saturation value, which remains above 70% for the duration of the experiments. The yeast exhibited an exponential growth period in the initial 24 h, until the glucose

was exhausted and the ethanol had reached its maximum concentration of 5.42 g/L. After glucose depletion, ethanol was utilized as a carbon source, resulting in ethanol depletion and an acetic acid peak concentration of 1.19 g/L at 50 h. After this time, the acetic acid was consumed. After 24 h, the yeast presented a slow growth period to reach a maximum biomass density of 7.9 g/L. Beta-carotene production started in the early exponential growth phase and continued throughout the cultivation period. The β-carotene production increased markedly when consuming the subproducts, reaching nearly 120 mg/L at the end of a 72 h cultivation period.

Fig. 5b shows the batch culture profiles with the initial glucose raised to 90 g/L. When compared to Fig. 5a the same trends are seen with regard to each component in the system. In addition, it can be noted that the β-carotene yield is comparable, 15.2 mg L^{-1} h^{-1} when charged with 20 g/L versus 15.4 mg L^{-1} h^{-1} when 90 g/L is used. These results are similar to those shown in Fig. 1, where flask experiments show similar yields in the 20 g/L and 100 g/L initial glucose cases. However, when comparing the productivities of the two systems, it can be seen that an increase in initial substrate concentration leads to a longer initial lag phase, a result shown in literature for various biochemical systems [48,49]. These longer cultivation times lead to a drop in the process productivity, 1.67 for the 20 g/L system versus 0.90 for the 90 g/L system, and thus an increase in initial substrate is not suitable for economically practical commercial implementation.

3.2. Inhibition studies

The performed experiments reveal that the substrate concentrations studied did not present any inhibition effect in the strain as the maximum growth rate remained roughly constant up to glucose concentrations of 200 g/L (data not shown). The effect of ethanol inhibition in the *S. cerevisiae* SM14 can be observed in Fig. 7a, where inhibition is seen for amounts of ethanol as low as 4.5 g/L. The growth rate is drastically affected with ethanol concentration higher than 30 g/L and completely inhibits the growth of the cells at 65 g/L. The acetic acid study is shown in Fig. 7b, which illustrates that cell growth is affected at low concentrations of acetic acid, equivalent to 2 g/L. At 8.6 g/L cell growth is completely inhibited by acetic acid.

Using these data, it is possible to determine a normalized functional form for the inhibition effect of ethanol (χ_E) and acetic acid (χ_A) on the growth rate of *S. cerevisiae* SM14 on glucose. It has been shown in literature that equations such as that shown in Eq. (22) have been used to fit cellular growth inhibition, where the toxicity parameter η is commonly found to be unity and the E_{crit} is the critical ethanol threshold beyond which there is no observable cell growth [50–52].

$$\mu_{obs} = \mu_{\max}\left(1 - \frac{E}{E_{crit}}\right)^{\eta} \tag{22}$$

For this work it was determined that this linear system would not accurately model the inhibition effects of ethanol and acetic acid due to their nonlinear behavior. The functions of ethanol and acetic acid inhibition used in this work were chosen as an extension of these linear models to higher order polynomial models of their respective concentration, as shown by Eqs. (23) and (24), to try and capture the nonlinearity of the inhibition data. The fits given by these models are shown as the red lines in Fig. 7a for ethanol and Fig. 7b for acetic acid, respectively.

$$\chi_E = 1 - 4.1 \times 10^{-6} \cdot E^3 + 1.4 \times 10^{-4} \cdot E^2 - 9.1 \times 10^{-3} \cdot E \tag{23}$$

$$\chi_A = 1 - 0.011 \cdot A^2 - 0.021 \cdot A \tag{24}$$

The maximum concentration of ethanol and acetic acid found in the bioreactor during cultivation was 5.4 g/L and 1.2 g/L, respectively. Based on the inhibition studies, we can determine that the ethanol reduces the maximum glucose growth rate by approximately 6.5% and the acetic acid inhibition results in a decrease of about 5.7%.

Table 1
Optimal parameter estimates for the batch kinetic models.

Parameter	Value	Units	Parameter	Value	Units
$\mu_{max,G}$	0.2516	h^{-1}	a_{AE}	1.0031	$\frac{g\ Cell}{g\ Ethanol}$
K_{SG}	0.4137	gGlucoseL^{-1}	Y_{XG}	0.1855	$\frac{g\ Cell}{g\ Glucose}$
$\mu_{max,E}$	0.0218	h^{-1}	Y_{XE}	0.3637	$\frac{g\ Cell}{g\ Ethanol}$
K_{SE}	0.5618	gEthanolL^{-1}	Y_{XA}	1.0163	$\frac{g\ Cell}{g\ Acetic\ Acid}$
$\mu_{max,A}$	0.0182	h^{-1}	α_1	0.7545	$\frac{mg\ Product}{g\ Glucose}$
K_{SA}	0.4506	gAcetic AcidL^{-1}	α_2	13.9280	$\frac{mg\ Product}{g\ Ethanol}$
a_{GE}	1.2964		α_3	1.1089	$\frac{mg\ Product}{g\ Acetic\ acid}$
a_{GA}	1.0318		β	0.2804	$\frac{mg\ Product}{g\ Cell \cdot hr}$
a_{EG}	1.0636		k_1	1.7300	$\frac{g\ Ethanol}{g\ Cell}$
a_{EA}	1.0058		k_2	0.0936	$\frac{g\ Acetic\ Acid}{g\ Cell}$
a_{AG}	1.0000		k_3	0.2937	$\frac{g\ Acetic\ Acid}{g\ Cell}$

3.3. Parameter estimation

The developed kinetic model equations (Eqs. (1) through (7)) contain a total of 22 model parameters, all of which were estimated by using the previously described parameter estimation algorithm and the batch culture time profiles are shown in Fig. 8. The values of the optimal parameters obtained from the parameter estimation are compiled in Table 1. The model simulation provided the coefficients of determination for each variable of R_X^2 =0.989, R_G^2 =0.998, R_P^2 =0.993, R_E^2 =0.995 and R_A^2 =0.807; these R^2 values show that the predictive model can represent the experimental data with high accuracy. It is useful to note that the model predicts only production of carotenoids to be non-growth associated during glucose utilization and highly growth associated during ethanol utilization, as seen by the parameter α_1 being zero and α_2 being two orders of magnitude larger than β at the optimal solution.

3.4. Local sensitivity analysis

The effect of each parameter and the initial values of the state variables was calculated and plotted as shown in Fig. 9. Fig. 9a illustrates the sensitivity of the variables with respect to Y_{xg}. The glucose shows a high sensitivity during the time period it is used in the cultivation and then the sensitivity decreases to zero. The minimum and maximum values of glucose sensitivity are 0 and 60. Then, we can say that the local sensitivity of the glucose with respect to the parameter Y_{xg} is $0 < S^{local} < 60$. The same analysis was done for all the inputs and results are summarized Table 2. Fig. 9b presents the effect of the initial condition of the ethanol on the profiles of the state variables, where the negative sensitivity values represent an inhibitory effect.

In Table 2, we highlight the inhibitory effects captured by the model at the optimal values when changes in ethanol and acetic acid initial conditions are made. The predicted final value of the β-carotene shows a high sensitivity for small changes in the values of Y_{xg}, Y_{xe}, or initial biomass concentration G_i. Changes in the parameters governing the biomass production from glucose and ethanol would be expected to have an effect on the carotenoid production as it is an intracellular product (highlighted in pink in Table 2). The parameter β, symbolizing the non-growth associated carotenoid production, is a very influential variable in the prediction of β-carotene production, so small changes in this parameter lead to a larger effect on the carotenoid estimates, as seen by the elevated sensitivity index for the product. Other state variables are affected by parameter changes to a much smaller degree, most notably the

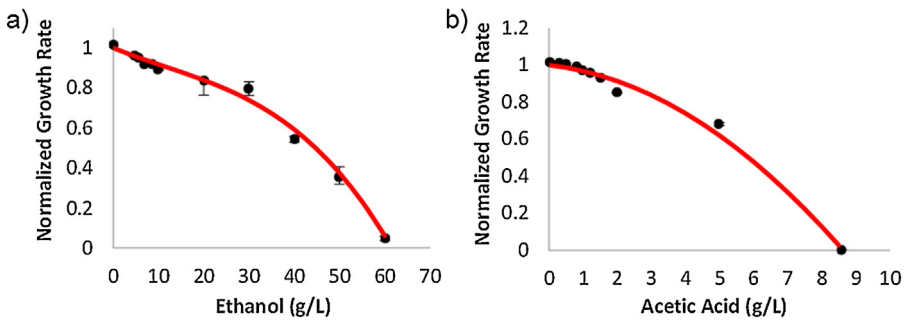

Fig. 7. The inhibition effect of (a) ethanol and (b) acetic acid sub-products on the growth rate of *S. cerevisiae* SM14 on glucose. Experimental data is represented by the markers and the obtained fit is denoted by the continuous red line. (For interpretation of the references to color in this figure legend, the reader is referred to the web version of this article.)

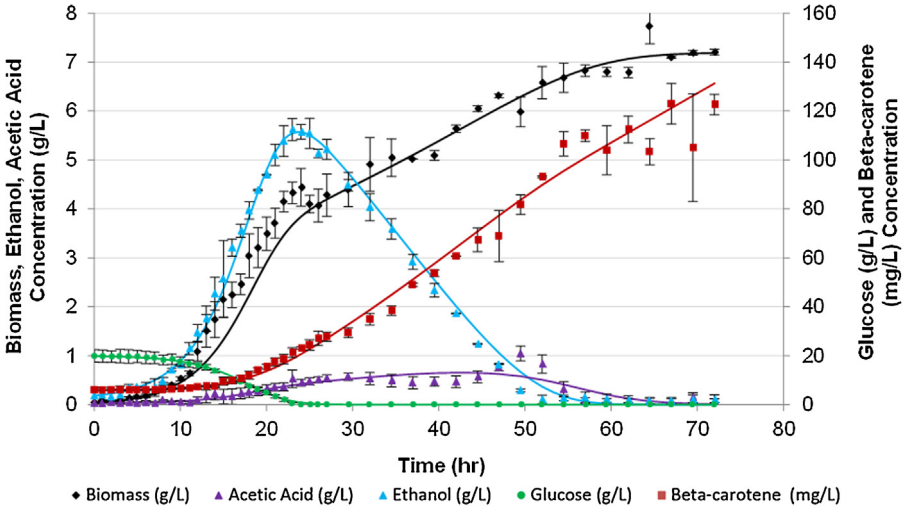

Fig. 8. Time profiles and curves of best fit for the cell growth, glucose consumption, ethanol and acetic acid concentration and carotenoids production in batch cultures of *S. cerevisiae* with 20 g/L initial glucose. Cultivation data are represented by the markers and the optimal fit by the solid lines.

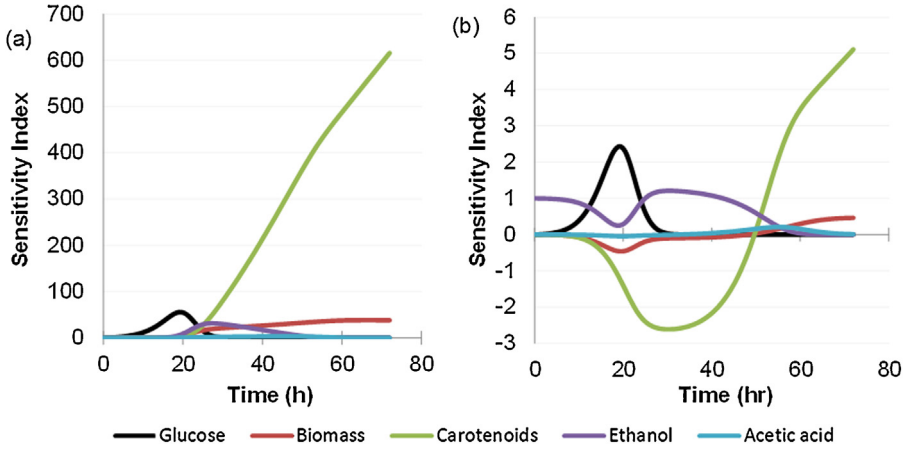

Fig. 9. Local sensitivity analysis of the models at the optimal solution for the (a) glucose yield with respect to biomass ($\boldsymbol{Y_{XG}}$) and (b) the initial concentration of ethanol ($\boldsymbol{E_i}$).

sensitivity of biomass, glucose and ethanol with respect to the Y_{XG} parameter (highlighted in orange in Table 2) and the biomass and ethanol with respect to the initial biomass inoculum X_i (highlighted in green in Table 2).

3.5. Global sensitivity analysis

Fig. 10 shows the relevant results from the global sensitivity analysis. In Fig. 10a we show that the global (S_y) and total (S_y^{tot}) sensitivity indices of all variables concerning biomass production were identical, thus we conclude that the variance in this model is not associated with any interaction between variables at any time. During the first 9 h, the biomass model is only influenced by the k_1 parameter representing the ethanol formation during glucose consumption. Between 9 and 25 h, the time pertaining to glucose consumption and ethanol and biomass production, the variance in the model outputs are due to both k_1 and Y_{xg}. After 50 h the Y_{xe}

Table 2
Minimum and maximum local sensitivity index values for each process variable with respect to all parameters and initial conditions. (For interpretation of the references to color in the text, the reader is referred to the web version of this article.)

	Biomass	Glucose	Ethanol	Acetic Acid	Carotenoids
X_i	1.0 < S < 35.	-170. < S < 0.0	-23 < S < 52.	-4.7 < S < 3.4	0.0 < S < 280
G_i	0.0 < S < 0.4	0.0 < S < 1.0	0.0 < S < 0.3	-	0.0 < S < 6.0
E_i	-0.5 < S < 0.5	0.0 < S < 2.4	0.0 < S < 1.2	0.0 < S < 0.2	-2.6 < S < 5.1
A_i	-0.5 < S < 1.0	0.0 < S < 2.4	-0.7 < S < 1.0	0.0 < S < 1.0	-6.5 < S < 2.4
P_i	-	-	-	-	-
Y_{XG}	0.0 < S < 40.	0.0 < S < 60.	-0.1 < S < 30.	-0.3 < S < 3.4	0.0 < S < 620
Y_{XE}	-0.1 < S < 8.4	0.0 < S < 0.4	0.0 < S < 11	0.0 < S < 2.8	0.0 < S < 140
Y_{XA}	0.0 < S < 1.0	-	0.0 < S < 0.2	0.0 < S < 0.5	-0.6 < S < 4.0
k_1	-	-	-	-	-
k_2	-0.4 < S < 3.7	0.0 < S < 2.2	-0.6 < S < 3.0	0.0 < S < 3.4	-14 < S < 16
k_3	0.0 < S < 2.4	0.0 < S < 0.1	0.0 < S < 1.0	0.0 < S < 1.5	-4.2 < S < 11
α_1	-	-	-	-	0.0 < S < 4.0
α_2	-	-	-	-	0.0 < S < 2.4
α_3	-	-	-	-	0.0 < S < 1.1
β	-	-	-	-	0.0 < S < 320

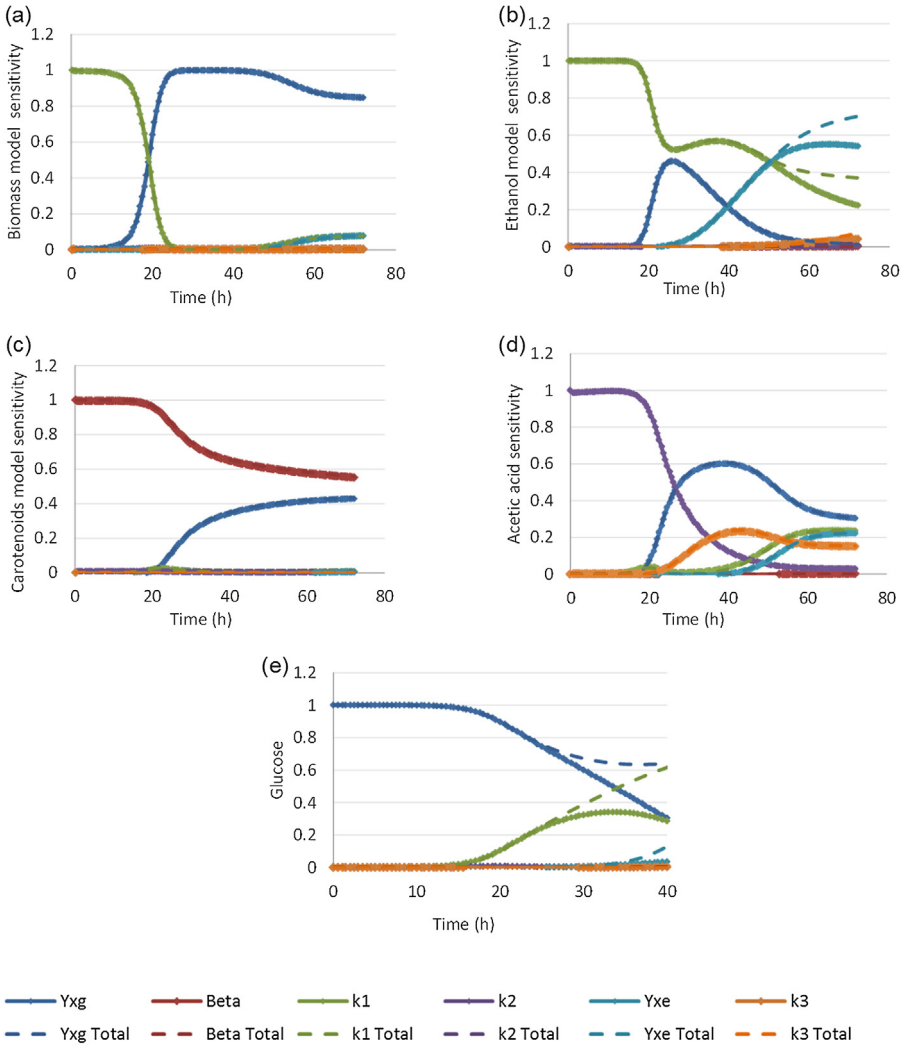

Fig. 10. Global sensitivity analysis of the (a) biomass, (b) ethanol, (c) carotenoids, (d) acetic acid, and (e) glucose models.

parameter begins to affect the variance in the biomass model as it is associated with ethanol consumption.

Ethanol formation and glucose consumption are related by the parameter k_1, leading to the only source of variance in the ethanol model during the time of ethanol production on glucose, as shown in Fig. 10b. Later, the ethanol is being consumed to form biomass and acetic acid, and the model variance begins to depend on the yield of biomass on glucose, Y_{xg}, the yield of biomass on ethanol, Y_{xe}, as well as the coefficients k_1 and k_3. At the end of the cultivation, interaction effects between k_1 and Y_{xe} are present, as seen in the divergence of the total global sensitivity from the individual global sensitivity.

The main source of variance in the β-carotene model through the first 16 h of the process was a result of the β parameter. As the cultivation progresses, the variance of the model shifts to depend on both β and Y_{xg}. The biomass formation is directly related with the substrate consumption, which is expressed in the models by the parameter Y_{xg}. The amount of β-carotene is then related to the amount of biomass through the non-growth association parameter β. Due to these interactions, after 16 h it is intuitive that these two parameters would play an important role in the model variance. Additionally, it can be seen that these two related parameters do not have any interaction effects on the model variance, as shown in Fig. 10c.

The global sensitivity analysis of acetic acid is shown in Fig. 10d. The acetic acid is present in the cultivation in small amounts compared to other variables and it is also affected by glucose, ethanol and biomass; this is reflected on the global sensitivity analysis results for acetic acid. Initially the variance in the model is due only to parameter k_2, which represents the acetic acid formation by glucose consumption. Later, the model variance is affected by the parameters associated with glucose and ethanol yield with respect to biomass (Y_{xg}, Y_{xe}), ethanol formation (k_2), and acetic acid formation due the ethanol depletion (k_3). The total sensitivity index represents the same global sensitivity effect on the acetic acid as the variables did; therefore we determine that the variance in the acetic acid model does not represent interaction with the related variables at any time.

The glucose model variance can be seen in Fig. 10e and shows results from the variance in the first 9 h depend on the yield of biomass on glucose, Y_{xg}, which is due the biomass formation during this period of the cultivation. Later, the variance of the model is due to both Y_{xg} and k_1; this is because of ethanol formation and during this time the global sensitivity shows the same effect as the total sensitivity. After the glucose is consumed, the total sensitivity differs from the global sensitivity, thus we conclude that the glucose model represents accurate information regarding interaction with the related variables.

The remaining variables Y_{xa}, α_1, α_2 and α_3 did not show any effect on the variance in the model predictions.

4. Conclusions

This study develops models and estimates the parameters necessary for accurately describing the growth of *S. cerevisiae* SM14 and the resulting product profiles, specifically glucose, ethanol, acetic acid, and β-carotene. Results indicate that the proposed model and estimated parameters are sufficient for describing the growth with glucose consumption and subproducts formation and depletion in batch cultures of *S. cerevisiae* SM14. Additionally, utilization of the coefficient of determination R^2 in the objective function provides a reliable optimal solution for parameter estimation of the model equations. It avoids the normalization of the equations or the weighting of them.

The local sensitivity analysis reflects the inhibition effect of the ethanol and acetic acid concentration in the system and also indicates for which parameters we must have accurate parameter estimation in order to develop a suitable description of the cultivation process. Global sensitivity analysis gives an understanding of the mathematical models in all the input space. The results show appropriate connections between the model variance, parameters of study, and characteristics of the cultivation process.

The methods presented here have a much wider application than the single case study of β-carotene production from genetically altered S. *cerevisiae*. Modified versions of these models and methods can be applied to any biological system for which there is a set of sub-products that experience generation and depletion through the course of a single batch fermentation. Additionally, the models described for this specific case study can be used in future optimization and controls studies, including applications in fed-batch and continuous production processes. Finally, knowledge of the *S. cerevisiae* kinetics is the first step toward the analysis large-scale production for which the economic impact of biologically produced nutraceuticals can be ascertained.

Acknowledgements

We would like to thank Michelle Olson for her additional assistance with this work.

Partial financial supports from the endowed Michael O'Connor Chair II and the Texas A&M University Institute for Advanced Studies are gratefully acknowledged.

References

[1] G.A. Armstrong, J.E. Hearst, Carotenoids 2: genetics and molecular biology of carotenoid pigment biosynthesis, FASEB J. 10 (1996) 228–237.
[2] D.A. Bender, Vitamin A: retinol and B-carotene, in: Nutritional Biochemistry of the Vitamin, Cambridge University Press, New York, 1995, pp. 19–49.
[3] R. Raja, S. Hemaiswarya, R. Rengasamy, Exploitation of Dunaliella for β-carotene production, Appl. Microbiol. Biotechnol. 74 (1991) 517–523.
[4] R.L. Ausich, Commercial opportunities for carotenoid production by biotechnology, Pure Appl. Chem. 69 (1997) 2169–2174.
[5] W.L. Marusich, J.C. Bauernfeind, Oxycarotenoids in poultry feeds, in: Carotenoids as Colorants and Vitamin A Precursors: Technological and Nutritional Applications, Academic Press, London, 1981.
[6] H.J. Nelis, A.P. De Leenheer, Microbial sources of carotenoid pigments used in foods and feed, J. Appl. Bacteriol. 70 (1991) 181–191.
[7] K.L. Simpson, T. Katayama, C.O. Chichester, Carotenoids in fish feeds, in: Carotenoids as Colorants and Vitamin A Precursors: Technological and Nutritional Applications, Academic Press, London, 1981.
[8] R. Edge, D.J. McGarvey, T.G. Truscott, The carotenoids as anti-oxidants—a review, J. Photochem. Photobiol. B41 (1997) 189–200.
[9] P.J. Hulshof, T. Kosmeijer-Schuil, C.E. West, P.C. Hollman, Quick screening of maize kernels for provitamin A content, J. Food Compos. Anal. 20 (2007) 655–661.
[10] P. Polazza, N.I. Krinsky, Antioxidant effects of carotenoids in vivo and in vitro: an overview, Methods Enzymol. 213 (1992) 403–420.
[11] G. Van Popel, R.A. Goldbohm, Epidemiologic evidence for beta-carotene and cancer prevention, Am. J. Clin. Nutr. 62 (1995) 291–296.
[12] G.I. Fregova, D.M. Beshkova, Carotenoids from *Rhodotorula* and *Phaffia*: yeast of biotechnological importance, J. Ind. Microbiol. Biotechnol. 36 (2009) 163–180.
[13] P. Vachali, P. Bhosale, P.S. Bernstein, Microbial carotenoids from fungi, Methods Mol. Biol. 898 (2012) 41–59.
[14] E. Johnson, W. Schroeder, Microbial carotenoids, Adv. Biochem. Eng. Biotechnol. 53 (1995) 119–178.
[15] P.C. Lee, C. Schmidt-Dannert, Metabolic engineering towards biotechnological production of carotenoids in microorganisms, Appl. Microbiol. Biotechnol. 60 (2002) 1–11.
[16] H. Crabtree, Observations on the carbohydrate metabolism of tumors, Biochem. J. 23 (3) (1929) 536–545.
[17] R. De Deken, The crabtree effect: a regulatory system in yeast, J. Gen. Microbiol. 44 (1966) 149–156.
[18] A. Fiechter, F.K. Gmünder, Metabolic control of glucose in yeast and tumor cells, Adv. Biochem. Eng. Biotechnol. 39 (1989) 1–28.
[19] B. Sonnleitner, O. Käppeli, Growth of Saccharomyces cerevisiae is controlled by its limited respiratory capacity: formulation and verification of a hypothesis, Biotechnol. Bioeng. 28 (6) (1986) 927–937.

[20] N. Paczia, A. Nilgen, T. Lehman, J. Gätgens, W. Wiechert, S. Noack, Extensive exometabolome analysis reveals extended overflow metabolism in various microorganisms, Microb. Cell Fact. 11 (2012) 122.
[21] B. Xu, M. Jahic, S.O. Enfors, Modeling of overflow metabolism in batch and fed batch cultures of Escherichia coli, Biotechnol. Progr. 15 (1) (1999) 81–90.
[22] Z. Amribt, H. Niu, P. Bogaerts, Macroscopic modeling of overflow metabolism in fed-batch cultures, Biochem. Eng. J. 70 (2013) 196–209.
[23] Y.S. Liu, J.Y. Wu, Modeling of *Xanthophyllomyces dendrorhous* growth on glucose and overflow metabolism in batch and fed-batch cultures for astaxanthin production, Biotechnol. Bioeng. 101 (5) (2008) 996–1004.
[24] C.H. Luna-Flores, J.J. Ramírez-Cordova, C. Pelayo-Ortiz, R. Fermat, E.J. Herrera-López, Batch and fed-batch modeling of carotenoids production by *Xanthophyllomyces dendrorhous* using *Yucca fillifera* date juice as substrate, Biochem. Eng. J. 53 (2010) 131–136.
[25] L.H. Reyes, J.M. Gomez, K.C. Kao, Improving carotenoids production in yeast via adaptive laboratory evolution, Metab. Eng. 21 (2014) 26–33.
[26] Michelle L. Olson, Metabolic Engineering of *S. cerevisiae* for Carotenoid Production Optimization (Master's thesis), Texas A&M University, 2014, Available electronically from: http://hdl.handle.net/1969.1/153880.
[27] H. Holzer, Regulation of carbohydrate metabolism by enzyme competition, Cold Spring Harbor Symposia on Quantitative Biology 26 (1961) 277–288.
[28] H. Holzer, H.W. Goedde, Zwei Wege von Pyruvate zu Acetyl-Coenzym A in Hefe, Biochem. Z. 329 (1957) 175–191.
[29] O. Käppeli, Regulation of carbon metabolism in *Saccharomyces cerevisiae* and related yeasts, Adv. Microb. Physiol. 28 (1987) 181–209.
[30] E. Postma, C. Verduyn, W.A. Scheffers, J.P. Van Dijken, Enzymic analysis of the Crabtree effect in glucose-limited chemostat cultures of *Saccharomyces cerevisiae*, Appl. Environ. Microbiol. 55 (1989) 468–477.
[31] M.K. Jacobson, C. Bernofsky, Mitochondrial acetaldehyde dehydrogenase from *Saccharomyces cerevisiae*, Biochim. Biophys. Acta (BBA) Enzymol. 350 (1974) 277–291.
[32] C. Wills, Regulation of sugar and ethanol metabolism in *Saccharomyces cerevisiae*, Biochem. Mol. Biol. 25 (4) (1990) 245–280.
[33] B. Özaydin, H. Burd, T.S. Lee, J.D. Keasling, Carotenoid-based phenotypic screen of the yeast deletion collection reveals new genes with roles in isoprenoid production, Metab. Eng. 1 (2013) 174–183.
[34] R. Verwaal, J. Wang, J.P. Meijnen, H. Visser, G. Sandmann, J.A. van den Berg, A.J.J. van Ooyen, High-level production of beta-carotene in *Saccharomyces cerevisiae* by successive transformation with carotenogenic genes from *Xantophyllomyces dendrorhous*, Appl. Environ. Microbiol. 73 (13) (2007) 4342–4350.
[35] V.M. Ye, S.K. Bhatia, Pathway engineering strategies for production of beneficial carotenoids in microbial host, Biotechnol. Lett. 34 (8) (2012) 1405–1414.
[36] B. Maiorella, W. Blanch, C.R. Wilke, By-product inhibition effects on ethanolic fermentation by *Saccharomyces cerevisiae*, Biotechnol. Bioeng. 25 (1983) 103–121.
[37] M.L. Shuler, F. Kargi, Bioprocess Engineering: Basic Concepts, Prentice Hall PTR, NJ, 2002.
[38] J. Monod, Recherches sur la croissance des cultures bactériennes (studies on the growth of bacterial cultures), Actua. Sci. Ind. 911 (1942) 1–215.
[39] H. Yoon, G. Klinzing, H.W. Blanch, Competition for mixed substrates by microbial populations, Biotechnol. Bioeng. 19 (1977) 1193–1210.
[40] X.M. Ge, F.W. Bai, Intrinsic kinetics of continuous growth and ethanol production of a flocculating fusant yeast strain SPSC01, J. Biotechnol. 124 (2006) 363–372.
[41] Y.S. Liu, J.Y. Wu, Perfusion culture process plus H2O2 stimulation for efficient astaxanthin production by *Xanthophyllomyces dendrorhous*, Biotechnol. Bioeng. 97 (3) (2007) 568–573.
[42] R. Luedeking, E.L. Piret, A kinetic study of the lactic acid fermentation Batch process at controlled pH, J. Biochem. Microbiol. Technol. Eng. 1 (4) (1959) 393–412.
[43] M.S. Krishnan, N.W.Y. Ho, G.T. Tsao, Fermentation kinetics of ethanol production from glucose and xylose by recombinant *Saccharomyces* 1400(pLNH33), Appl. Biochem. Biotechnol. 78 (1–3) (1999) 373–388.
[44] C.H. Reinsch, Smooth by spline functions, Numer. Math. 10 (3) (1967) 177–183.
[45] A. Varma, M. Morbidelli, H. Wu, Parametric Sensitivity in Chemical Systems, Cambridge University Press, Cambridge, UK, 1999.
[46] I.M. Sobol', Global sensitivity indices for nonlinear mathematical models and their Monte Carlo estimates, Math. Comput. Simul 55 (2001) 271–280.
[47] A. Saltelli, M. Ratto, T. Andres, F. Campolongo, J. Cariboni, D. Gatelli, M. Saisana, S. Tarantola, Global Sensitivity Analysis, John Wiley & Sons Ltd., West Sussex, England, 2008.
[48] I.A.M. Swinnen, K. Bernaerts, E.J.J. Dens, A.H. Geeraerd, J.F. Van Impe, Predictive modelling of the microbial lag phase: a review, Int. J. Food Microbiol. 94 (2004) 137–159.
[49] B. Atkinson, F. Mavituna, Biochemical Engineering and Biotechnology Handbook, The Nature Press, Surrey, England, 1984.
[50] A.-P. Zeng, et al., Multiple product inhibition and growth modeling of Clostridium butyricum and Klebsiella pneumoniae in glycerol fermentation, Biotechnol. Bioeng. 44 (1994) 902–911.
[51] K.-K. Cheng, H.-J. Liu, D.-H. Liu, Multiple growth inhibition of Klebsiella pneumoniae in 1,3-propanediol fermentation, Biotechnol. Lett. 27 (2005) 19–22.
[52] N.S. Khan, I.M. Mishra, R.P. Singh, B. Prasad, Modeling the growth of Corynebacterium glutamicum under product inhibition in L-glutamic acid fermentation, Biochem. Eng. J. 25 (2005) 173–178.